STRENGTH OF ALUMINUM UNDER COMPRESSION IN A SHOCK

S. M. Bakhrakh, A. G. Ivanov, N. P. Kovalev, V. N. Mineev, G. P. Simonov, E. S. Tyun'kin, and N. P. Khokhlov

UDC 532.593;539.374

Shock-wave attenuation in metals is studied in a number of papers [1-8] in order to obtain information about the strength of substances behind a shock front. A number of experiments on the high-velocity deformation of metals are not successfully described within the framework of an elastic–plastic model with constant yield point, and dislocation models [9-13] are relied upon for the interpretation of experimental data.

The strength properties of an aluminum alloy D16 under shock compression pressures from 8 to 20 kbar are investigated experimentally and numerically in this paper. The possibility of describing experimental results on the damping of an elastic forerunner and a plastic wave on the basis of the model of an elastic–plastic body and a model based on the representations of dislocation dynamics is investigated.

1. Formulation of the Tests and Methodology of the Experiment

Plane shocks were produced in targets of l =1-40 mm thickness by collisions with a Δ =0.9-mm-thick impactor at a velocity of w=275 m/sec. The spread in the quantity w from test to test was 10% on the average. The impactor and target were fabricated from a D16 alloy as delivered. The collisions were executed in a ballistic shock tube analogous to that described in [14]. The parameters of the one-dimensional shock in the target were studied by the method of capacitive [15, 16], quartz [17], and Manganin [18, 19] transducers. The diversification of the collisions in the 70-mm-diameter domain did not exceed 0.13 μsec, and ~0.02 μsec in the domain of transducer mounting.

Quartz disks of 10 and 20 mm diameter and 2 and 4 mm thickness were used to record the pressure profile. The quartz transducer was hooked up in a short-circuit loop with the R=91-Ω load resistance. The recording time was 0.35 and 0.7 μsec, and corresponded to the transit time T of an elastic shock over the quartz thickness. The piezomodulus of the X-cut quartz was taken to be $2.04 \cdot 10^{-8}$ C/kbar·cm^2 for $p_{n1} \leq 6$ kbar and $2.15 \cdot 10^{-8}$ C/kbar·cm^2 in the 9-16-kbar range [20]. Records from the quartz transducer carry information about the pressure distribution in the wave ~0.03 μsec with a time resolution, which permits clarification of the elastic–plastic wave structure.

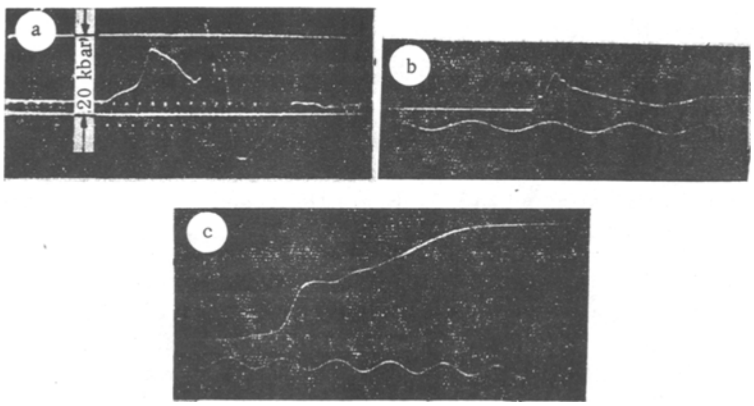

Fig. 1

Moscow. Translated from Zhurnal Prikladnoi Mekhaniki i Tekhnicheskoi Fiziki, No. 2, pp. 137-143, March-April, 1980. Original article submitted May 4, 1979.

0021-8944/80/2102-0271$07.50 © 1980 Plenum Publishing Corporation

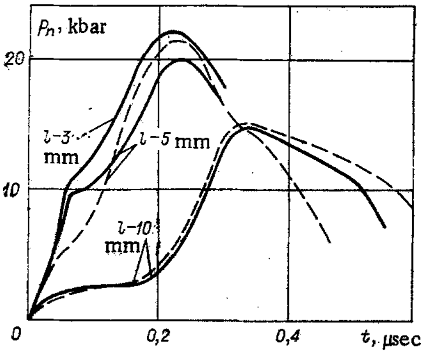

Fig. 2

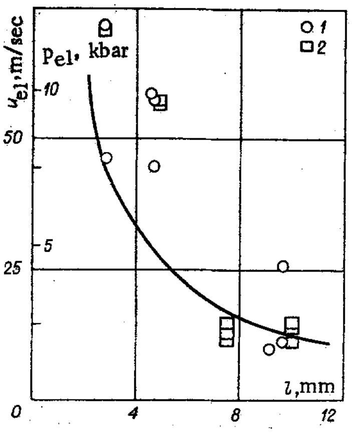

Fig. 3

The Manganin pressure transducer was a plane rectangular grating wound from 0.05-mm-diameter Manganin wire (mark MNMtsZ-12 All-Union State Standard (GOST) 492-52) on a 10 × 10 mm area. The transducer thickness was 0.15 mm, which corresponds to a time resolution of 0.25 μsec. The piezoresistive coefficient of Manganin was taken to be $2.3 \cdot 10^{-3}$ kbar^{-1} for $p_n \leq 15$ kbar, and $2.7 \cdot 10^{-3}$ for $p_n > 15$ kbar [19].

Recording of the instantaneous velocity of the specimen free-surface motion was by a capacitor transducer of 0.78-cm^2 area hooked up in a short-circuit loop (R = 98 Ω).

Oscilloscopes with a passband ~20 MHz were used to record the electrical signals from the transducers.

2. Test Results and Discussion

Oscillograms illustrating the pressure change in the shock (Fig. 1a, quartz pressure transducer, l = 10 mm, timing markers 0.1 μsec, T = 0.7 μsec) and the specimen free-surface motion velocity (Fig. 1b, c, capacitor transducers, l = 5 and 30 mm, respectively, timing markers 1.0 μsec) are presented in Fig. 1.

The experimental compression wave profiles recorded by a quartz pressure transducer (averaged from the results of three to four tests) are presented in Fig. 2 (solid lines). The profiles recorded have a two-wave configuration. The first wave is elastic and propagated at the speed c_e = 6.2 ± 0.1 km/sec, and the second, plastic, wave has the velocity c_w = 5.3 ± 0.2 km/sec in the domain under investigation.

The experimental results illustrating the change in pressure p_{el} (points 1) and mass flow rate u_{el} (points 2) on the elastic wavefront are presented in Fig. 3 as a function of target thickness. A substantial diminution in the pressure amplitude is detected in the elastic wave from 12 to 2 kbar as the specimen thickness increased from 3 to 10 mm. Attenuation of the elastic precursor was observed earlier in aluminum [21], Armco iron [22], and silicon [23]. Let us note the well-defined spread in the experimental points that is possibly associated with the high sensitivity of the precursor amplitude to the material microstructure.

The plastic wavefront being recorded (Fig. 2) is noticeably smoothed out. For l = 10 mm the time of wavefront rise is ~0.2 μsec, which agrees with the results in [5] obtained by a laser interferometer method for aluminum under shock compression to 21 kbar.

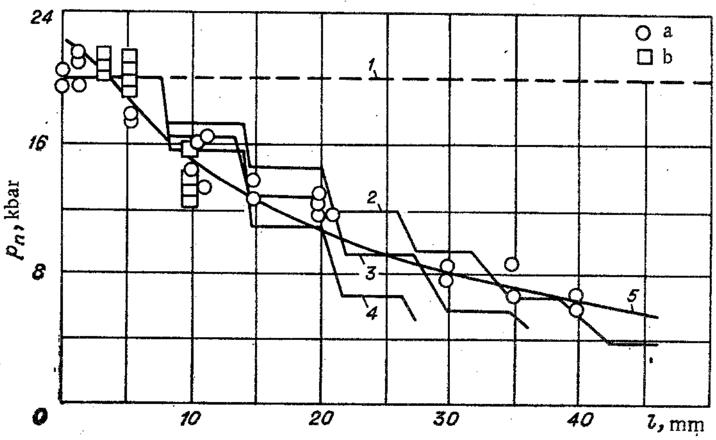

Fig. 4

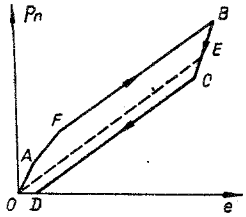

Fig. 5

The two-wave structure of the unloading wave is fixed on the p(t) profiles for l =10 mm. According to the model of an ideal elastic–plastic medium, the amplitude of the elastic section of the unloading wave Δp should be twice the amplitude of the elastic precursor. In experiments, the quantity was $\Delta p \simeq 1.3 p_{el}$. It can be assumed that one of the possible reasons for such a discrepancy could be the Bauschinger effect for shock compression and the subsequent plastic unloading [5]. This effect can be explained from the aspect of dislocation theory; in fact the finite velocity of the motion and multiplication of dislocations and its associated delay in fluidity result in the dynamic yield point in a plastic compression wave being several times greater than its static value. At the same time, an increase in the number of dislocations in the compression wave results in the reverse passage from elasticity to plasticity proceeding at a significantly lower tangential stress during expansion of the shock compressed material.

Data on the damping of the plastic wave amplitude as it moves over the target are presented in Fig. 4 curve a gives results of measurements by the Manganin transducer, and curve b by the quartz transducer). Pressure pulse propagation cannot be described from the viewpoint of a hydrodynamic approximation (curve 1, computed by the method in [4]). Shock attenuation turns out to be stronger than follows from the hydrodynamic model. Curves 2-4 correspond to plastic wave damping by the model of an elastic–plastic medium [1] with elastic unloading wave amplitudes of 3, 4, and 5 kbar, respectively. Comparing curves 2-4 with the results of the experiment shows that the damping of the plastic shock in the 8-20 kbar range is described by the model of an elastic–plastic medium with an elastic unloading wave amplitude Δp=3-5 kbar, where the amplitude of the elastic section of the unloading diminishes as the wave propagates.

Extrapolation of the experimental results to l = 0 (see Fig. 4) yields p_n = 23-24 kbar for the initial pressure. The initial shock amplitude, computed by the formula $p_n = \rho_0 c_e u$ is ~22 kbar. It is therefore impossible to exclude that a purely elastic, or an almost elastic, nature of the collision is realized in the initial instant [23, 24].

3. Model of a Medium. Results of Computations

In the interest of comparison with the experiments described, computations were performed on an electronic computer for a complicated model of a medium based on the representations of dislocation dynamics. The problem of the collision of two plates under uniaxial strain-state conditions was examined. The equations of motion have the form

$$\frac{dx}{dt} = u, \frac{d\rho}{dt} = -\rho \frac{\partial u}{\partial x}, \frac{du}{dt} = -\frac{1}{\rho}\frac{\partial p}{\partial x} + \frac{2}{3\rho}\frac{\partial s}{\partial x}, \tag{3.1}$$

where x is the Eulerian coordinate of the particle, u is the velocity, ρ is the density, p is the hydrodynamic pressure, and s is the intensity of the stress tensor deviator. Let us note that $p_n = p - {}^2/_3 s$.

The system (3.1) is closed by equations governing the properties of the medium.

The equation of state was taken in the form

$$p = \frac{\rho_0 c_0^2}{n}\left[\left(\frac{\rho}{\rho_0}\right)^n - 1\right] \tag{3.2}$$

with the following values of the parameters: $\rho_0 = 2.7$ g/cm^3, $c_0 = 5.3$ km/sec, and $n = 2.5$. The governing relationships for the stress deviator were taken in the form

$$\frac{ds}{dt} = 2G\left(\frac{\partial \varepsilon}{\partial t} - 2\frac{\partial \varepsilon^p}{\partial t}\operatorname{sgn} s\right); \tag{3.3}$$

$$\frac{\partial \varepsilon^p}{\partial t} = bu_* N \exp\left[-2\tau_*/|s|\right]; \tag{3.4}$$

$$\frac{dN}{dt} = m\frac{\partial \varepsilon^p}{\partial t}, \quad N(0) = N_0, \tag{3.5}$$

where G is the shear modulus, $\partial\varepsilon/\partial t = \partial u/\partial x$ is the total strain rate, $2\partial\varepsilon^p/\partial t$ is the plastic strain rate, N is the density of mobile dislocations, N_0 is the initial density of the mobile dislocations, m is the multiplication factor, b is the Burgers vector, τ_* is the characteristic shear resistance, and $u_* = (G/\rho)^{1/2}$ is the shear speed of sound.

The plastic strain rate is determined by the internal dislocation parameters just until it becomes equal to the total strain rate according to (3.4). Afterwards it is natural to assume that the plastic strain rate equals the total shear strain rate (or is less if hardening is introduced). It is assumed that $2\partial\varepsilon^p/\partial t = \partial\varepsilon/\partial t$ if

$$\partial\varepsilon/\partial t < 2bu_* N \exp\left[-2\tau_*/|s|\right]. \tag{3.6}$$

Then $ds/dt = 0$ and $s = \text{const}$.

For $|s| < Y_s$ it is assumed $\partial\varepsilon^p/\partial t = 0$. The behavior of the medium is purely elastic here, being subject to Hooke's law in differential form

$$ds/dt = 2G\partial\varepsilon/\partial t. \tag{3.7}$$

The unloading was also considered elastic. The shear modulus was calculated by the formula

$$G = \frac{3\rho_0 c_w^2 (1 - 2\nu)}{2(1 + \nu)}. \tag{3.8}$$

The method of pseudoviscosity was used to compute the shocks. The countable blurring of the shocks can result in additional multiplication of the dislocations on the front of the elastic precursor. In this connection, multiplication of the dislocations, defined by (3.5), was allowed in the computation scheme only behind the elastic wavefront, and the front localization was made by means of the position of the first maximum of the countable viscosity.

The following were taken as dislocation parameters: $b = 2.86 \cdot 10^{-8}$ cm, $N_0 = 2 \cdot 10^6/\text{cm}^2$ [21], $u_* = 2.8$ km/sec, $m = 40 \cdot 10^9/\text{cm}^2$. It was assumed that $Y_s = 0.5$ kbar, the coefficient τ_* was selected numerically from a comparison between the computational and experimental data. The best agreement was reached for $\tau_* = 1$ kbar.

The behavior of a material subject to the equations of the medium (3.2)-(3.8) during shock compression and subsequent expansion is shown schematically in Fig. 5 in the coordinates p_n, the compressive stress in the strain direction, and the compression e. Here OA is the elastic-strain section, AF is the "yield lag" section, FB is the plastic loading section, BC is the elastic unloading curve, CD is the plastic unloading curve, and OE is the hydrostatic compression curve.

This model differs from the ideal elastic–plastic medium [4, 26] in the presence of the yield lag section when the density of the mobile dislocations is not enough to transfer the material into the flowing state. The dynamic yield point at which the material arrives is determined by the magnitude of this section which can be varied for different processes. The diagram is nonsymmetric relative to the hydrostatic compression curve. This asymmetry diminishes as the wave advances and attenuates.

The system (3.1)-(3.8) was solved numerically by finite differences. The computation method based on splitting according to physical processes is elucidated in [27]. The size of the calculation cell is 0.05-0.1 mm.

The computed profiles of $p_n(t)$ are denoted by dashes in Fig. 2. Let us note the good correspondence between the computed and experimental curves for l = 10 mm. The amplitude of the elastic unloading wave measured in test was 3.5 kbar for this specimen thickness, which corresponds to the estimate obtained for the quantity Δp obtained from an analysis of shock attenuation according to [1].

The computed curve obtained for attenuation of the elastic wave amplitude is presented in Fig. 3. The location of the precursor was determined in the numerical computation for a comparison with the experimental data by means of the local minimum of the slope $p_n(x)$. Qualitative agreement between the experimental and computed data on elastic precursor attenuation can be asserted, while the quantitative correspondence can be acknowledged as satisfactory.

The computed curve for attenuation of the plastic wave amplitude is presented in Fig. 4 (curve 5). Plastic wave attenuation is transmitted well enough in the computation.

It can therefore be concluded that the plastic deformation model considered mainly reflects the singularity in the behavior of aluminum under shock compression to 20 kbar and subsequent unloading.

LITERATURE CITED

1. D. R. Curran, "Nonhydrodynamic attenuation of shock waves in aluminum," J. Appl. Phys., 34, No. 9 (1963).
2. J. O. Erkman and A. B. Christensen, "Attenuation of shock waves in aluminum," J. Appl. Phys., 38, No. 13 (1967).
3. S. A. Novikov and L. M. Sinitsyna, "On the influence of shock compression pressure on the magnitude of critical shear stresses in metals," Zh. Prikl. Mekh. Tekh. Fiz., No. 6 (1970).
4. L. V. Al'tshuler, M. P. Brazhnik, and G. S. Telegin, "Strength and elasticity of iron and copper at high shock compression pressures," Zh. Prikl. Mekh. Tekh. Fiz., No. 6 (1971).
5. L. M. Barker, "Fine structure of compressive and release wave shapes in aluminum measured by the velocity interferometer technique," Preprints of Symp. on High Dynamic Pressure, Paris, Sept. 11-15, 1967.
6. A. A. Vorob'ev, A. N. Dremin, and G. I. Kanel', "Dependence of the aluminum elasticity coefficients on degree of compression in a shock," Zh. Prikl. Mekh. Tekh. Fiz., No. 5 (1974).
7. P. J. A. Fuller and J. H. Price, "Dynamic stress-strain release paths for aluminum and magnesium measured to 200 kV," Brit. J. Appl. Phys., 2, Ser. 2 (1969).
8. A. N. Dremin and G. I. Kanel', "Compression and rarefaction waves in shock compressed metals," Prikl. Mekh. Tekh. Fiz., No. 2 (1976).
9. D. D. Gilman, "Dislocation dynamics and behavior of materials under shock action," in: Mechanics [Russian translation], No. 2 (1970).
10. J. N. Johnson and L. M. Barker, "Dislocation dynamics and steady plastic wave profiles in 6061-T6 aluminum," J. Appl. Phys., 40, No. 11 (1969).
11. R. I. Nigmatulin and N. N. Kholin, "Yield lag and hardening in the high-speed deformation of metals," Dokl. Akad. Nauk SSSR, 209, No. 1 (1973).
12. R. I. Nigmatulin, P. B. Vainshtein, N. N. Kholin, N. Kh. Akhmadeev, and V. P. Myasnikov, "Numerical modeling of physicochemical processes and shock propagation in solids and composites," in: Numerical Methods of the Mechanics of Continuous Media [in Russian], Vol. 7, No. 2, Novosibirsk (1976).
13. A. I. Gulidov, V. M. Fomin, and N. N. Yanenko, "Compression wave structure in inelastic media," Izv. Akad. Nauk SSSR, Mekh. Tverd. Tela, No. 5 (1975).
14. G. R. Fowles, G. E. Duvall, J. Asay, P. Bellamy, F. Fristman, D. Grady, T. Mitchaels, and R. Mitchell, "Gas gun for impact studies," Rev. Sci. Instrum., 41, No. 7 (1970).
15. A. G. Ivanov and S. A. Novikov, "Capacitive transducer method for recording the instantaneous velocity of a moving surface," Prib. Tekh. Eksp., No. 1 (1963).
16. M. H. Rice, "Capacitor technique for measuring the velocity of a plane conducting surface," Rev. Sci. Instrum., 32, No. 4 (1961).

17. O. E. Jones, F. W. Neilson, and W. B. Benedick, "Dynamic field behavior of explosively loaded metals determined by a quartz transducer technique," J. Appl. Phys., 33, No. 11 (1962).
18. P. J. A. Fuller and J. H. Price, "Dynamic pressure measurements to 300 kbar with resistance transducer," Brit. J. Appl. Phys., 15, No. 6 (1964).
19. G. I. Kanel', "Application of Manganin transducers to measure the shock compression pressure of condensed media," Preprint Inst. Khim. Fiz. Akad. Nauk SSSR, Chernogolovka (1973).
20. R. A. Graham, F. W. Neilson, and W. B. Benedick, "Piezoelectric current from shock-loaded quartz in a submicrosecond stress gauge," J. Appl. Phys., 36, No. 5 (1965).
21. T. E. Arwidsson, Y. M. Gupta, and G. E. Duvall, "Precursor decay in 1060 aluminum," J. Appl. Phys., 46, No. 10 (1975).
22. J. W. Taylor and M. H. Rice, "Elastic properties of iron," J. Appl. Phys., 34, No. 2 (1963).
23. Yu. N. Tyunyaev and V. N. Mineev, "Elastic stress relaxation mechanism in the shock compression of doped silicon," Fiz. Tverd. Tela, 17, No. 10 (1975).
24. Y. M. Gupta and G. R. Fowles, "Shock-induced dynamic yielding in lithium fluoride single crystals. Metallurgical effects at high strain rates," AIME, New York–London (1973).
25. R. Richtmayer and K. Morton, Difference Methods of Solving Boundary-Value Problems [Russian Translation], Mir, Moscow (1972).
26. M. L. Wilkins, "Analysis of elastic–plastic flows," in: Computational Methods in Hydrodynamics [Russian translation], Mir, Moscow (1967).
27. S. M. Bakhrakh and N. P. Kovalev, "Application of the splitting method to analyze elastic–plastic flows," Trans. of the Second All-Union Conference on Numerical Methods of Solving Problems of the Theory of Elasticity and Plasticity [in Russian], Novosibirsk (1971).

SIMILARITY AND THE ENERGY DISTRIBUTION IN AN EXPLOSION IN AN ELASTIC–PLASTIC MEDIUM

P. F. Korotkov and B. M. Prosvirnina

UDC 539.3

An exact solution of the problem of an explosion in a solid medium where large strains occur is possible by using numerical methods [1, 2]. Results of computations of separate versions of strong explosions are presented in [3-9]. The spherically symmetric explosion is investigated in a medium which differs minimally in complexity of the description from an elastic medium but an important property of a medium subjected to large strains, the capacity to plastic flow, is taken into account for a detailed analysis and to obtain general regularities in this paper. Such an ideal elastic–plastic medium differs from the elastic by one excess parameter, the yield point. The problem of an explosion in such a medium was approximately solved earlier for simplifying assumptions, and a detailed survey is found in [10-14].

The equations of motion continuity and energy in Lagrange variables for the nonstationary motion of a continuous medium with spherical symmetry have the form

$$\frac{\rho_0}{V}\frac{\partial v}{\partial t}=\frac{\partial \sigma_r}{\partial r}+2\frac{\sigma_r-\sigma_\varphi}{r},$$

$$\frac{1}{V}\frac{\partial V}{\partial t}=\frac{1}{r^2}\frac{\partial}{\partial r}(r^2 v),\quad V=\frac{\rho_0}{\rho},$$

$$\rho_0\frac{\partial E}{\partial t}=-p\frac{\partial V}{\partial t}+V\left(S_r\frac{\partial e_r}{\partial t}+2S_\varphi\frac{\partial e_\varphi}{\partial t}\right),$$

$$\frac{\partial e_r}{\partial t}=\frac{\partial v}{\partial r},\ \frac{\partial e_\varphi}{\partial t}=\frac{v}{r},\quad \sigma_r=-p+S_r,\ \sigma_\varphi=-p+S_\varphi,$$

where v is the velocity, ρ is the density of the medium, ρ_0 is the initial density, p is the pressure, σ_r and σ_φ are the radial and tangential stresses, S_r and S_φ are stress deviator components, E is the internal energy of the medium per unit mass, and e_r and e_φ are strain tensor components.

The relationships between the stresses and strains for an elastic material are used in the form

Moscow. Translated from Zhurnal Prikladnoi Mekhaniki i Tekhnicheskoi Fiziki, No. 2, pp. 143–152, March–April, 1980. Original article submitted April 9, 1979.

0021-8944/80/2102-0276$07.50